ELSEVIER

Electric Power Systems Research 62 (2002) 93–103

ELECTRIC POWER SYSTEMS RESEARCH

www.elsevier.com/locate/epsr

Controlled series compensation in coordination with double order SVS auxiliary controller and induction M/C for repressing the torsional oscillations in power systems

Sushil Kumar Gupta [a,*], Narendra Kumar [b], A.K. Gupta [a]

[a] *C.R. State College of Engineering, Murthal, Sonepat, India*
[b] *Delhi College of Engineering, Delhi, India*

Received 27 June 2001; received in revised form 12 December 2001; accepted 13 December 2001

Abstract

Development of high voltage and high current rated power semiconductor devices has led to the flexible ac transmission systems (FACTs). This paper deals with the controlled series compensation for enhancing the power transfer capability of transmission line in coordination with SVS (double order static var system) auxiliary controller and induction machine for repressing the torsional oscillations in power systems. The IEEE first benchmark model is considered for study. The role of controlled series compensation is mainly to repress large power oscillations while that of induction machine is to damp low power perturbations. The SVS auxiliary controller has a significant effect on both. Computer simulations show that the proposed scheme is effective in repressing the torsional oscillations for all levels of series compensation over a wide range of operating conditions. © 2002 Published by Elsevier Science B.V.

Keywords: Controlled series compensation; Flexible ac transmission system; Static–var system

1. Introduction

Recently, a lot of research work has been directed towards devising methods for better utilization of the transmission lines of the power systems. The concept of flexible ac transmission systems (FACTs) is made possible due to advances in power electronics technology. The thyristor controlled series compensation (TCSC) is one possible way to implement FACTs concepts. This can be realized by inserting controllable series compensator on the transmission line, which modulates the line impedance. The compensation of line may lead to the phenomenon of subsynchronous resonance that may cause the shaft failures. Many counter measures have been reported to damp out SSR oscillations. A linearized discrete time model of a series compensated transmission line is presented by A. Ghosh and G. Ledwich [1]. In the study, thyristor controlled reactor is used as the compensating device. Study shows that the dynamics of the transmission line is governed by the change in the line reactance. Narendra Kumar and M.P. Dave [2] have incorporated the CSC having bang–bang control characteristics to improve the transient performance. But this paper does not show the effect of controller on SSR oscillations. S.S. Choi et al. [3] proposed a compensator having a combination of thyristor switched capacitors and a thyristor controlled reactor. But the control of these devices for damping SSR has not been demonstrated. Hak-Gun Han et al. [4] performed the analysis of thyristor controlled series compensator dynamics using the state variable approach but the analysis for the torsional oscillation has not been investigated. A linear

* Corresponding author.

0378-7796/02/$ - see front matter © 2002 Published by Elsevier Science B.V.
PII: S0378-7796(02)00022-6

optimal controller has been designed and demonstrated in [5] to implement variable series compensations in transmission networks to damp inertia oscillations but the control scheme is valid only for a specific operating condition, and it is complex and difficult to implement for continuously variable load. Ning Yan et al. [6] show the design of controller that can modulate the impedance of line for enhancing the damping of oscillations. But the results show that the controller does not damp all the modes. J.V. Milanovic and I.A. Hiskens [7] proposed the robust tuning of static var compensation, but the result shows the inter-area mode is less damped when one load had uncertain parameters. This paper investigates the effect of controlling of series capacitor in coordination with the double order reactive power SVS auxiliary controller and an induction machine for repressing the torsional oscillations. The SSR modes are very successfully and effectively damped out. The induction machine mechanically coupled to the high-pressure turbine is found effective for suppressing the high frequency-low magnitude torsional oscillations while the controlled series capacitor is effective for suppressing the low frequency high magnitude torsional oscillations. Double order reactive power SVS auxiliary controller enhances the damping of both, low as well as high magnitude, oscillations.

2. System model

The IEEE first bench-mark model [8] is considered for analysis. The configuration of the system, under study as shown in Fig. 1, consists of a generator feeding power to an infinite bus through a series compensated transmission line. The SVS is connected to the bus near to the receiving end. The compensation of transmission line is done near to the sending end bus. It has been observed that SVS connected at the middle of the transmission line is not able to stabilize the oscillations produced due to the compensating capacitor presented towards load end, which limits the level of series compensation of line. The differential equations describing constituent subsystems, —i.e. the generator, excitation, transmission, SVS and T-G set are summarized below for the sake of completeness.

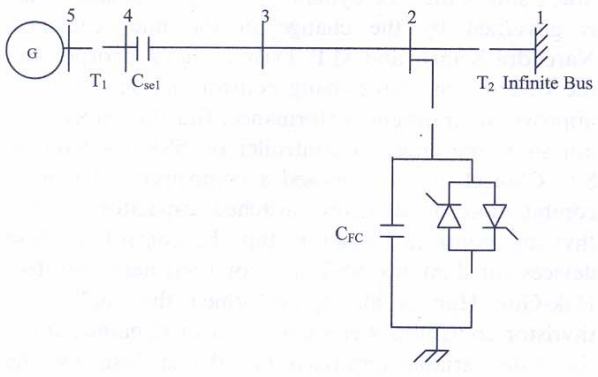

Fig. 1. Schematic diagram of system under study.

2.1. Generator model

The detailed mathematical model [9] of the synchronous machine, used here, includes the field winding (f) and a damper winding (h) along the d-axis and two damper windings (g, k) along q-axis. The rotor flux linkages are defined as follows:

$$\frac{dX_1}{dt} = a_1X_1 + a_2X_2 + b_2\cos\,\delta X_{23} - b_2\sin\,\delta X_{32} - b_1X_{17} \quad (1)$$

$$\frac{dX_2}{dt} = a_3X_1 + a_4X_2 + b_3\cos\,\delta X_{23} - b_3\sin\,\delta X_{32} \quad (2)$$

$$\frac{dX_3}{dt} = a_5X_3 + a_6X_4 + b_5\sin\,\delta X_{23} + b_5\cos\,\delta X_{32} \quad (3)$$

$$\frac{dX_4}{dt} = a_7X_3 + a_8X_4 + b_6\sin\,\delta X_{23} + b_6\cos\,\delta X_{32} \quad (4)$$

The coefficients a_i and b_i are given in [9].

2.2. Mechanical system model

A study of torsional interactions between turbine generator shaft systems requires a detailed modeling of the mechanical system. The turbo generator mechanical system is represented as a linear multi mass spring dash–pot system as shown in Fig. 2. Each major rotating element is modeled as a lumped mass represented
by its inertia while every shaft element is modeled as a mass less rotational spring with its stiffness expressed by the spring constant. The equations of motions of the rotating system are summarized from Eqs. (5)–(17).

$$\frac{dX_5}{dt} = X_{11} - \omega_0 \quad (5)$$

$$\frac{dX_6}{dt} = X_{12} - \omega_0 \quad (6)$$

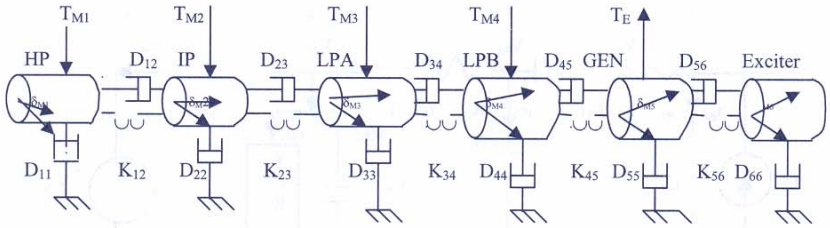

Fig. 2. Six mass representation of mechanical system.

$$\frac{dX_7}{dt} = X_{13} - \omega_0 \tag{7}$$

$$\frac{dX_8}{dt} = X_{14} - \omega_0 \tag{8}$$

$$\frac{dX_9}{dt} = X_{15} - \omega_0 \tag{9}$$

$$\frac{dX_{10}}{dt} = X_{16} - \omega_0 \tag{10}$$

$$\frac{dX_{11}}{dt} = \left(\frac{1}{M_1}\right) \times (-(D_{11} + D_{12})(X_{11} - \omega_0) + D_{12}(X_{12} - \omega_0) - K_{12}(X_5 - X_6) + T_{M1} - T_{im1}) \tag{11}$$

$$\frac{dX_{12}}{dt} = \left(\frac{1}{M_2}\right) \times (D_{12}(X_{11} - \omega_0) - (D_{12} + D_{22} + D_{23})(X_{12} - \omega_0) + D_{23}(X_{13} - \omega_0) - K_{12}(X_6 - X_5) - K_{23}(X_6 - X_7) + T_{M2}) \tag{12}$$

$$\frac{dX_{13}}{dt} = \left(\frac{1}{M_3}\right) \times (D_{23}(X_{12} - \omega_0) - (D_{23} + D_{33} + D_{34})(X_{13} - \omega_0) + D_{34}(X_{14} - \omega_0) - K_{23}(X_7 - X_6) - K_{34}(X_7 - X_8) + T_{M3} \tag{13}$$

$$\frac{dX_{14}}{dt} = \left(\frac{1}{M_4}\right) \times (D_{34}(X_{13} - \omega_0) - (D_{34} + D_{44} + D_{45})(X_{14} - \omega_0) + D_{45}(X_{15} - \omega_0) - K_{34}(X_8 - X_7) - K_{45}(X_8 - X_9) + T_{M4} \tag{14}$$

$$\mathrm{elc}T = Xd'_2(X_{23}XII_Q - X_{32}XII_D) \tag{15}$$

$$\frac{dX_{15}}{dt} = \left(\frac{1}{M_5}\right) \times (D_{45}(X_{14} - \omega_0) - (D_{45} + D_{55} + D_{56})(X_{15} - \omega_0) + D_{56}(X_{16} - \omega_0) - K_{45}(X_9 - X_8) - K_{56}(X_9 - X_{10}) - \mathrm{elc}T) \tag{16}$$

$$\frac{dX_{16}}{dt} = \left(\frac{1}{M_6}\right) \times (D_{56}(X_{15} - \omega_0) - (D_{56} + D_{66})(X_{16} - \omega_0) - K_{56}(X_{10} - X_9)) \tag{17}$$

2.3. Exciter model

The IEEE type-1 continuously acting regulating excitation system [10] is used. Differential equations describing the excitation system are as follows:

$$S_E = A_E \cdot e^{(B_E \cdot X_{17})} \tag{18}$$

$$\frac{dX_{17}}{dt} = -\frac{(K_E + S_E)X_{17}}{T_E} + \frac{X_{19}}{T_E} \tag{19}$$

$$\frac{dX_{18}}{dt} = -\frac{K_F(K_E + S_E)X_{17}}{T_E T_{FF}} + \frac{K_F X_{19}}{T_E T_{FF}} - \frac{X_{18}}{T_{FF}} \tag{20}$$

$$\frac{dX_{19}}{dt} = -\frac{K_A X_{18}}{T_A} - \frac{X_{19}}{T_A} - \frac{K_A XV_{gg}}{T_A} + \frac{K_A V_{refE}}{T_A} \tag{21}$$

2.4. Transmission line model

The transmission line is represented by a nominal π-model of a long line. Fig. 3 shows the α-axis representation of the AC network. SVS is connected near to load

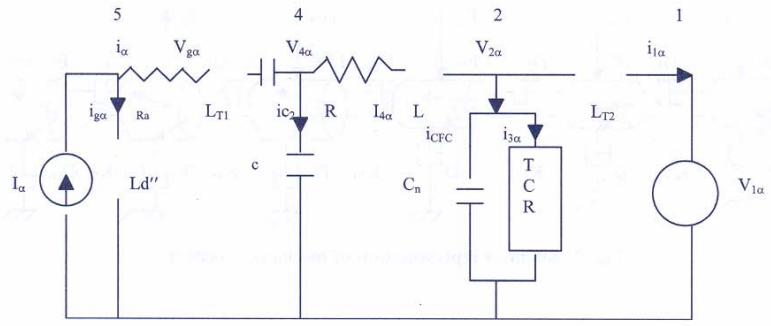

Fig. 3. α-Axis representation of the network.

bus and the controlled capacitor at the sending end side. Linear differential equations after transforming to d, q, axes are presented from Eqs. (22)–(39).

$$\frac{dX_{20}}{dt} = \left(\frac{1}{L_{T2}}\right)X_{24} - \omega_0 \cdot X_{29} - \left(\frac{1}{L_{T2}}\right)V_{1D} \tag{22}$$

$$\frac{dX_{21}}{dt} = \left(\frac{1}{L_{T2}}\right)X_{24} - \omega_0 \cdot X_{30} - \left(\frac{1}{L_{T2}}\right)V_{1D} \tag{23}$$

$$\frac{dX_{22}}{dt} = \left(\frac{-R}{L}\right)X_{22} - \frac{X_{25}}{L} + \frac{X_{26}}{L} - \omega_0 \cdot X_{31} \tag{24}$$

$$\frac{dX_{23}}{dt} = \left(\frac{-R_a}{L_A}\right)X_{23} - \frac{X_{26}}{L_A} - \frac{X_{28}}{L_A} - \omega_0 \cdot X_{32} - \left(\frac{\omega_0 L'_{D2}}{L_A}\right)XII_Q - \left(\frac{L'_{D2}}{L_A}\right)II_D \tag{25}$$

$$\frac{dX_{24}}{dt} = -\frac{X_{21}}{C_n} + \frac{X_{22}}{C_n - \omega_0}\frac{X_{33} - X_{38}}{C_n} \tag{26}$$

$$\frac{dX_{25}}{dt} = -\frac{X_{21}}{C_n} + \frac{X_{22}}{C_n - \omega_0}\frac{X_{34} - X_{38}}{C_n} \tag{27}$$

$$\frac{dX_{26}}{dt} = -\frac{X_{22}}{C} + \frac{X_{23}}{C} - \omega_0 \cdot X_{35} \tag{28}$$

$$\frac{dX_{27}}{dt} = \frac{X_{21}}{C_{se2}} - \omega_0 \cdot X_{36} \tag{29}$$

$$\frac{dX_{28}}{dt} = \frac{X_{23}}{C_{se1}} - \omega_0 \cdot X_{37} \tag{30}$$

$$\frac{dX_{29}}{dt} = \omega_0 \cdot X_{20} + \frac{X_{33}}{L_{T2}} - \left(\frac{1}{L_{T2}}\right)V_{1Q} \tag{31}$$

$$\frac{dX_{30}}{dt} = \omega_0 \cdot X_{21} + \frac{X_{33}}{L_{T2}} - \left(\frac{1}{L_{T2}}\right)V_{1Q} \tag{32}$$

$$\frac{dX_{31}}{dt} = \omega_0 \cdot X_{22} - \left(\frac{R}{L}\right)X_{31} - \frac{X_{34}}{L} + \frac{X_{35}}{L} \tag{33}$$

$$\frac{dX_{32}}{dt} = \omega_0 \cdot X_{23} - \left(\frac{R_a}{L_A}\right)X_{32} - \frac{X_{35}}{L_A} - \frac{X_{37}}{L_A} + \left(\frac{\omega_0 L'_{D2}}{L_A}\right)XII_D - \left(\frac{L'_{D2}}{L_A}\right)II_Q \tag{34}$$

$$\frac{dX_{33}}{dt} = \omega_0 \cdot X_{24} - \frac{X_{30}}{C_n} + \frac{X_{31}}{C_n} - \frac{X_{39}}{C_n} \tag{35}$$

$$\frac{dX_{34}}{dt} = \omega_0 \cdot X_{25} - \frac{X_{30}}{C_n} + \frac{X_{31}}{C_n} - \frac{X_{39}}{C_n} \tag{36}$$

$$\frac{dX_{35}}{dt} = \omega_0 \cdot X_{26} - \frac{X_{31}}{C} + \frac{X_{32}}{C} \tag{37}$$

$$\frac{dX_{36}}{dt} = \omega_0 \cdot X_{27} + \frac{X_{30}}{C_{se2}} \tag{38}$$

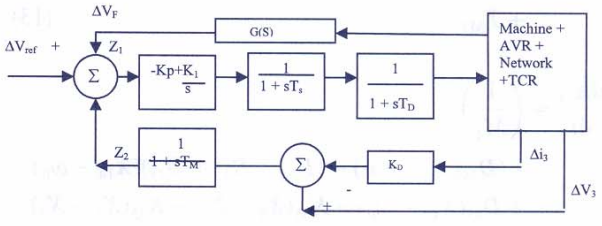

Fig. 4. SVS control system with auxiliary feedback.

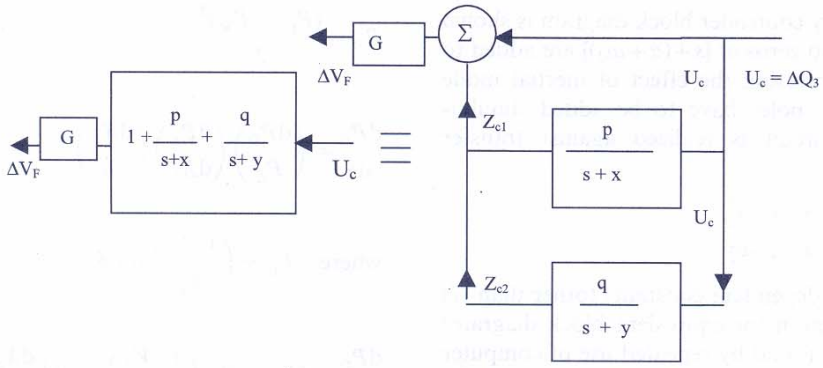

Fig. 5. Auxiliary controller block diagram.

$$\frac{dX_{37}}{dt} = \omega_0 \cdot X_{28} + \frac{X_{32}}{C_{sel}} \quad (39)$$

2.5. SVS model

The SVS has been employed to an increasing extent in the modern power systems due to its capability of VAR generation and absorption. SVS can maintain the voltage deviation within close tolerance, and causes enhancement of dynamic performance of the system. The block diagram of a general SVS control system [2] is as shown in Fig. 4. The state and output equations of the system are obtained as (Eqs. (40)–(45)).

$$\frac{dX_{38}}{dt} = \left(\frac{-1}{Q}\right)(X_{15}X_{38} - \omega_0 i_{3D}) + \omega_0 i_{3Q} - X_{15}X_{39} + X_{15}X_{25}X_{43} - \omega_0 V_{3D}B_0 + \omega_o V_{3D}(X_{43} - B_0) \quad (40)$$

$$\frac{dX_{39}}{dt} = \left(\frac{-1}{Q}\right)(X_{15}X_{39} - \omega_0 i_{3Q}) - \omega_0 i_{3D} + X_{15}X_{38} + X_{15}X_{34}X_{43} - \omega_0 V_{3Q}B_0 + \omega_0 V_{3Q}(X_{43} - B_0) \quad (41)$$

$$\frac{dX_{40}}{dt} = -X_{41} + V_{ref} - \sqrt{(X_{25}^2 + X_{34}^2)} + \Delta V_F \quad (42)$$

$$\frac{dX_{41}}{dt} = \frac{-X_{41}}{T_M} + \left(\frac{1}{T_M}\right)\left(\sqrt{(X_{25}^2 + X_{34}^2)} - V_3\right) + \left(\frac{K_D}{T_M}\right) \times \left(i_3 - \sqrt{(X_{38}^2 + X_{39}^2)}\right) \quad (43)$$

$$\frac{dX_{42}}{dt} = \left(\frac{-1}{T_S}\right)X_{42} - \left(\frac{K_I}{T_S}\right)X_{40} + \left(\frac{K_P}{T_S}\right)X_{41} - \left(\frac{K_P}{T_S}\right)V_{ref} + \left(\frac{K_P}{T_S}\right)\sqrt{(X_{25}^2 + X_{34}^2)} - \left(\frac{K_P}{T_S}\right)\Delta V_F \quad (44)$$

$$\frac{dX_{43}}{dt} = \frac{X_{42}}{T_D} - \frac{(X_{43} - B_0)}{T_D} \quad (45)$$

3. Coordinated controllers

Double order auxiliary controller's output is used as the auxiliary signal to the input of the SVS. The overall transfer function of the system is adjusted to enhance the damping of torsional oscillations. Controlled series compensation is the novel technique proposed under the flexible ac transmission system. The CSC scheme has been simulated by step-wise control of the degree of series compensation to the control of power flow, which ultimately improves the stability of the power system. An induction machine coupled with the high-pressure turbine of mechanical system acts as a motor or generator depending upon its slip during the torque disturbances, this enhances the system damping. All these controllers have been applied simultaneously to achieve the satisfactory performance.

3.1. Double order auxiliary controller

Double order SVS auxiliary controller has been considered as corrective subsystem to compensate the phase lag between the SVS input and output susceptance, and thereby, increases the margin of stability of

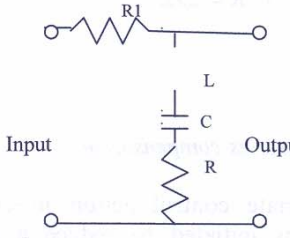

Fig. 6. Realization of circuit for the controller of Fig. 5.

the system. Auxiliary controller block diagram is shown in Figs. 5 and 6. Two zeros at $[s+(\alpha+\omega_d)]$ are added to the system for suppressing the effect of inertial mode of the system. Two poles have to be added simultaneously and the circuit is realized against transfer function:

$$T.F. = \frac{S^2 + 2\alpha S + \alpha^2 + \omega_d^2}{S_2 + 2\beta S + \alpha^2 + \omega_d^2}$$

There are three independent constants (other than G) in this transfer function (or equivalent block diagram) which are optimally found by repeated use of computer program. The constants are presented in Appendix B.7.2.

Here $y = (\alpha^2 + \omega_d^2)/x$,

$$p = ((x-\alpha)^2 + \omega_d^2)/(y-x),$$

$$q = ((y-\alpha)^2 + \omega_d^2)/(x-y).$$

Deviation in reactive power (ΔQ_3) at the SVS bus has been used as the auxiliary input signal. Differential equations for auxiliary controller are found from Eqs. (46)–(49).

$$U_c = \Delta Q_3 = V_{3D}(X_{31} - i_{4Q}) + i_{4Q}(X_{25} - V_{3D}) - V_{3Q}(X_{22} - i_{4D}) - i_{4D}(X_{34} - V_{3Q}) \quad (46)$$

$$\Delta V_F = G(U_c + X_{44} + X_{45}) \quad (47)$$

$$\frac{dX_{44}}{dt} = -xX_{44} + pU_c \quad (48)$$

$$\frac{dX_{45}}{dt} = -yX_{45} + qU_c \quad (49)$$

where $R_1 = -L(p+q)$,

$\alpha = [x + y + (p+q)]/2$,

$C = 1/L(\omega_d^2 + \alpha^2)$, $R = 2\alpha L$

3.2. Controlled series compensation

The appropriate control action in control series compensation is initiated to reduce a function P_D (defined below) progressively, following the disturbance.

$$P_D = \frac{(P_E - P_M)^2}{2} \quad (50)$$

$$\frac{dP_D}{dt} = \left(\frac{dP_D}{P_E}\right)\left(\frac{dP_E}{dX_S}\right)\left(\frac{dX_S}{dt}\right) \quad (51)$$

where $P_E = \left(\frac{V_S V_1}{X_S}\right)\sin\delta$ (52)

$$\frac{dP_D}{dt} = (P_M - P_E)\left(\frac{V_S V_1}{X_S^2}\right)\sin\delta\left(\frac{dX_S}{dt}\right) \quad (53)$$

For

$$P_M > P_E, \quad \frac{dP_D}{dX_S} > 0 \quad (54)$$

Therefore, dX_s/dt should be less than zero, which means X_s should reduce with time and vise versa. A control scheme for controlling a bank of series capacitors is shown in Fig. 7. High power gate turn off thyristor valves are proposed to be used as power switches because of their ability to provide continuous variation of the compensation level. GTO-CSC switches have potential advantages over controlled series capacitor technologies using conventional thyristors.

Net level of series compensation is given by:

$$-jX_{sel} = \frac{-jX_c jX_r}{jX_r - jX_c} = -j\frac{X_c + X_c^2}{X_r - X_c} \quad (55)$$

$$X_r = \frac{\pi X_L}{\sigma - \sin\sigma} \quad (56)$$

$$X_c = X_{c1} + X_{c2} + X_{c3} + X_{c4} + X_{c5} \quad (57)$$

Hence, overall level of series compensation may be increased by reducing X_r and can be decreased by the switch capacitors. Application of controlled series

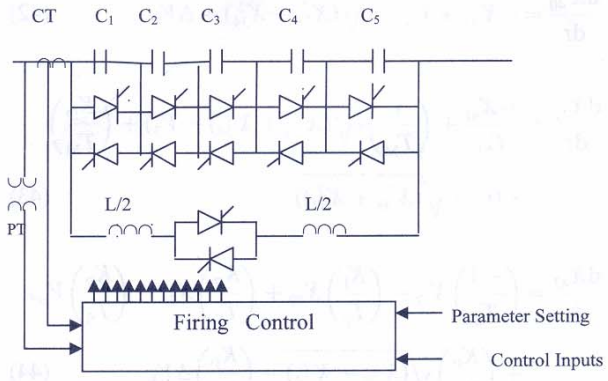

Fig. 7. Control series compensation scheme.

compensation is made for large disturbance. As disturbance occurs, CSC is employed to minimize the deviation of shaft angle, δ_{M5}. When the value δ is restored close to the pre disturbance value, CSC is taken out of action. Net level of series compensation is considered to be the function of generator's shaft angle and generator's velocity as shown in Eq. (58).

$$X_{sel} = X_{sel0}(1 + \sin(k_2(\delta + k_3(x(15) - \omega_0) - \delta_{M5}) \quad (58)$$

The constants k_2 and k_3 are given in section a.7.1.

3.3. Induction machine action

The property of induction M/C to act as a generator (when s is -ve) or motor (when s is +ve) is utilized to absorb the mechanical power when there is an excess and to release when there is a deficiency of it. Since this machine comes into operation during transients only, it is designed for very short-term rating, consequently machine has low inertia, low power and small size. Because of its small mass and tight coupling with the high pressure turbine it has been considered a single mass unit with HP turbine. It is observed that this machine takes care of low magnitude perturbations. Such a specially designed M/C may be named as Low Magnitude Induction Perturbation Shocker (LM-IPS). An approximate equivalent circuit of induction M/C has been taken. Electrically it is connected to the generator bus. The per unit torque of induction machine (T_{im1}) is given by:

$$T_{im1} = \frac{3r_2' s}{\omega_0(r_2' + (sx_2')^2)} \quad (59)$$

And slip is defined as

$$s = \frac{\omega_0 - x_{(11)}}{\omega_0} \quad (60)$$

4. Case study

The study system consists of two synchronous generators, which are represented by a single equivalent unit of 1110 MVA, at 22 kV. The electrical power is supplied to an infinite bus over 400 kV, 600 km long transmission line. A 55% series compensation of the line is being considered at the sending end. Compensation of the line can be controlled from 10 to 70% during transients. Controlling of compensation remains in action till the deviation in mechanical angle is restored to 1.5% of its pre disturbance value. The bank of compensating capacitors and parallel reactor is controlled as described in Section 3.2. The SVS is capable to supply 650 Mvar reactive power and is located at the receiving end side of the transmission line. It delivers 850 MVA load at the normal operating condition. The detailed system data are given in Appendix B.

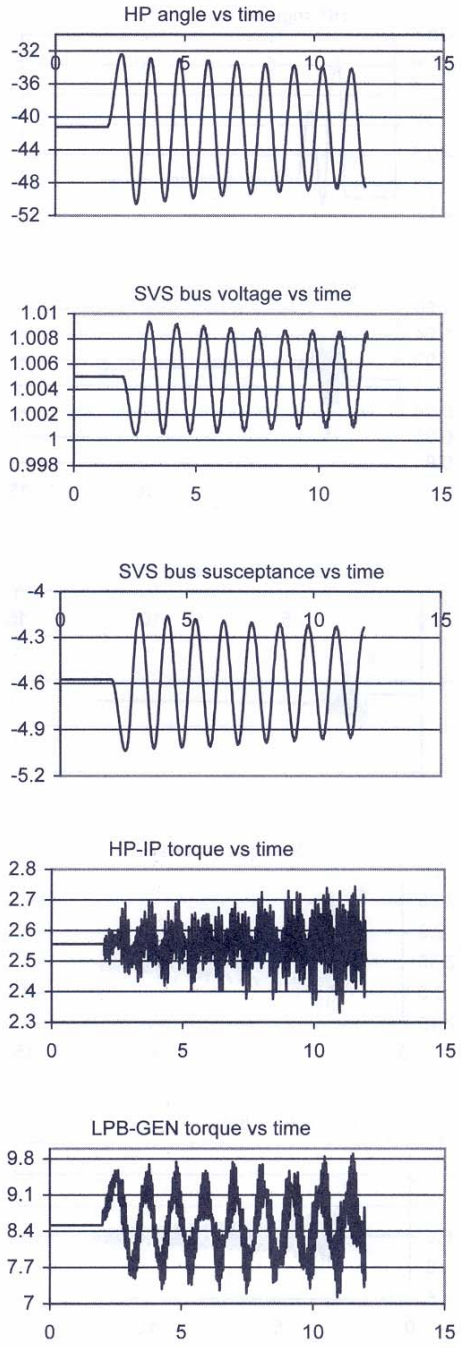

Fig. 8. System responses without auxiliary controlled scheme for 30% torque disturbance for 0.6 s at 55% compesation of line.

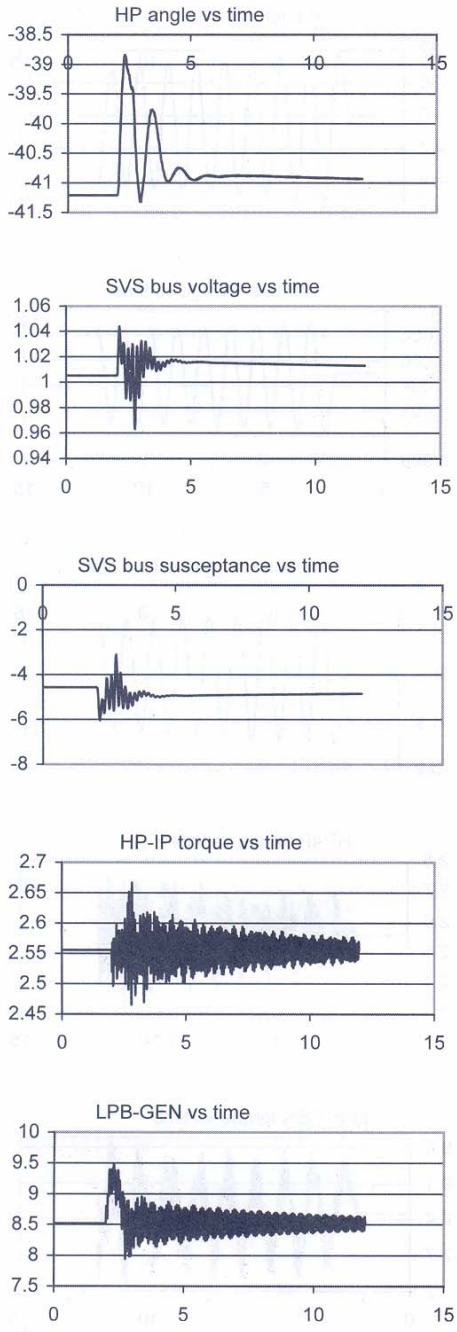

Fig. 9. System responses with auxiliary controlled scheme for 30% torque disturbance for 0.6 s at 55% compensation of line.

5. Simulation results

Digital time domain simulations for the system under large disturbances have been taken on the basis of non-linear differential equations with all non-linearities and limits considered. The load flow study is carried out for calculating the operating point. A fourth order Runge–Kutta method has been used for solving the non-linear

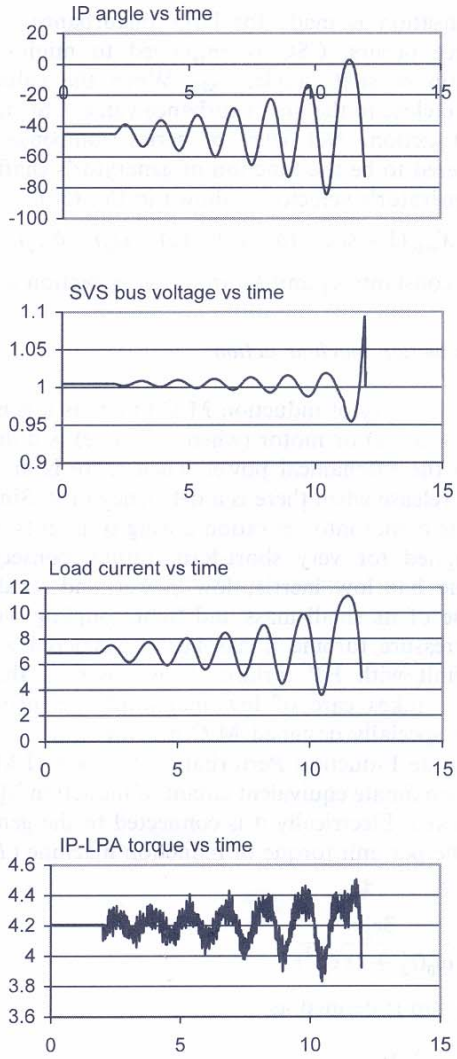

Fig. 10. System responses without auxiliary controlled scheme for 35% torque disturbance for 0.2 s at 25% compensation of line.

differential equations. System's natural damping is considered to be equal to zero so that the effect of controlling-scheme can be examined exclusively. Disturbance is simulated by 30% sudden increase in input torque for 0.6 s. The dynamic responses of the system without the coordinated approach are plotted in Fig. 8, there the torsional oscillations are unstable. Fig. 9 shows the responses of the system with the coordinated approach of the controllers. When coordinated approach of the controller is incorporated, satisfactory damped responses are achieved. Controlled series compensation in coordination with double order SVS auxiliary controller and induction machine can provide the sufficient torque to repress the torsional oscillations. Response curves at 25% series compensation of transmission line for 750 MVA load for 35% torque

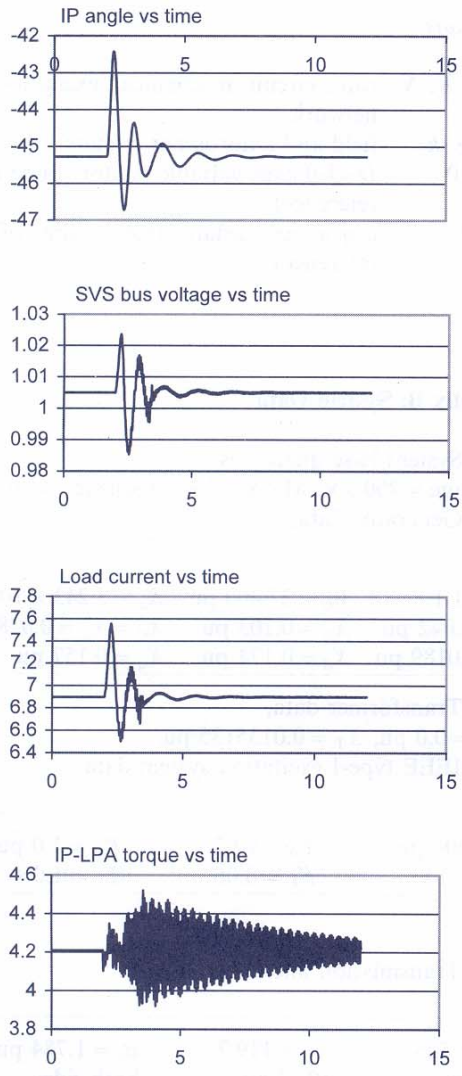

Fig. 11. System responses with auxiliary controlled scheme for 35% torque disturbance for 0.2 s at 25% compensation of line.

disturbance for 0.2 s without and with auxiliary controlled scheme are shown in Figs. 10 and 11, respectively. It is seen from Figs. 10 and 11 that the frequency oscillations rise progressively in magnitude without any auxiliary controller. When a proposed combination is applied, the power oscillations and torsional torque's oscillations are effectively damped out. Similar response curves are obtained for other levels of series compensation over wide operating conditions.

6. Conclusions

In this paper, a controlled series compensation in coordination with double order SVS auxiliary controller and induction m/c is proposed for repressing the torsional oscillations in power systems. Digital simulation results show that the damping effect of the proposed scheme is excellent. The role of controlled series compensation is to suppress large power oscillations while that of the induction machine is to damp out small perturbations. Double order auxiliary SVS controller adds to the damping in both large as well as small power oscillations. A calculation of advance shaft angle has been done for finding the appropriate level of series compensation. The controller is applicable for different levels of series compensation over a wide range of load variation.

Appendix A: Nomenclature

$X_1 = \psi_f$
$X_2 = \psi_h$
$X_3 = \psi_g$
$X_4 = \psi_k$
ψ_x shows the flux associated with the coil of rotor circuit represented by its subscripts
i_d and i_q are the d-axis and q-axis components of the machine terminal currents.
$X_5 = \delta_{M1}$ mech. delta1
$X_6 = \delta_{M2}$ mech. delta2
$X_7 = \delta_{M3}$ mech. delta3
$X_8 = \delta_{M4}$ mech. delta4
$X_9 = \delta_{M5}$ mech. delta5
$X_{10} = \delta_{M6}$ mech. delta6
$X_{11} = \omega_1$
$X_{12} = \omega_2$
$X_{13} = \omega_3$
$X_{14} = \omega_4$
$X_{15} = \omega_5$
$X_{16} = \omega_6$
δ_{Mi}, ω_i show the angular position and angular speed of the ith inertia
$X_{17} = V_f$
$X_{18} = V_S$
$X_{19} = V_r$
V_g generator terminal voltage
S_E saturation function
V_f excitation voltage of gen.
V_S stabilizing feedback signal voltage
V_r regulator's output voltage [10]
$X_{20} = i_{1D}$
$X_{21} = i_{2D}$
$X_{22} = i_{4D}$
$X_{23} = i_D$
$X_{24} = V_{2D}$
$X_{25} = V_{3D}$
$X_{26} = V_{4D}$
$X_{27} = V_{5RCD}$
$X_{28} = V_{6D}$

$X_{29} = i_{1Q}$
$X_{30} = i_{2Q}$
$X_{31} = i_{4Q}$
$X_{32} = i_{Q}$
$X_{33} = V_{2Q}$
$X_{34} = V_{3Q}$
$X_{35} = V_{4Q}$
$X_{36} = V_{5RCQ}$
$X_{37} = V_{6Q}$
$X_{38} = i_{3D}$
$X_{39} = i_{3Q}$

V_i, i_i are voltages and currents at buses or at circuit parameters in the network

V_{5RC} is the voltage at the capacitor (if connected) at receiving end

$X_{40} = Z_1$
$X_{41} = Z_2$
$X_{42} = Z_3$
$X_{43} = B$

Z_1, Z_2, Z_3 are regulator block input, measurement unit output and regulator block output

B susceptance offered by SVS

$X_{44} = Z_{C1}$
$X_{45} = Z_{C2}$

Z_{c1}, Z_{c2} are auxiliary controller system's states

ω_o normal frequency

B_o normal susceptance of SVS

P_E electrical power output from generator

P_M mechanical power input to the generator

X_c capacitive reactance of compensated capacitor

X_r reactance of controlled reactance

X_{sc1} net series compensation

σ conduction angle of the GTO of the controlled reactor

δ, θ, R, L power angle, bus angle, resistance, inductance

T_M, T_E mechanical, electrical torques

K_P, K_I proportional, integral gains of SVS voltage controller

G gain of SVS auxiliary controller

K_D slope of control characterstics

T_S, T_D, T_M firing delay, thyristor delay, measurement time constant

V_F auxiliary control signals

II_D, II_Q D and Q axis component of I_α current

HP high pressure turbine

IP intermediate pressure turbine

LPA low pressure turbine A

LPB low pressure turbine B

GEN generator

EXC exciter

Subscripts

R, M, E, N rotor circuit, mechanical, excitation, network

F, h, g, k field and amortisseur circuits

D, Q, 0 D-Q-0 axes variable (stator frame of reference)

d, q, 0 d-q-0 axes variable (rotor frame of reference)

Appendix B: System Data

B.1 System base quantities,
voltage = 400 kV, MVA = 100, frequency = 50.
B.2 Generator data.

$S_n = 11.1$	$V_n = 22\backslash 400$ pu	$R_a = 3.243 \times 10^{-4}$
$X'_d = 0.042$ pu	$X'_q = 0.103$ pu	$X''_d = x''_q = 0.0281$ pu
$X_l = 0.0189$ pu	$X_d = 0.174$ pu	$X_q = 0.157$ pu

B.3 Transformer data,
$R_T = 0.0$ pu, $X_T = 0.0135135$ pu.
B.4 IEEE type-I excitation system data.

$K_A = 400$ pu	$T_A = 0.02$ s	$K_E = 1.0$ pu
$T_E = 1.0$ s	$K_F = 0.06$	$T_F = 1.0$ s

B.5 Transmission line data.

$R = 12.525 \times 10^{-3}$ pu	$X_L = 119.7 \times 10^{-3}$ pu	$B_c = 1.784$ pu on both sides

B.6 SVS data, $Q = 100$.

$K_I = 1200$	$K_P = -1$	$K_D = 0.01$ pu
$T_M = 2.4$ ms	$T_s = 5$ ms	$T_D = 1.667$ ms

B.7 Controllers data.
B.7.1 Series compensation:
For 55% compensation of line impedance; $k_2 = 3$, $k_3 = 0.01$s and for 25% compensation of line impedance; $k_2 = 2$, $k_3 = 0.01$s. $X_L = 11.66\%$, $X_{c1} = 10\%$, $X_{c2} = 25\%$, $X_{c3} = 40\%$, $X_{c4} = 55\%$, $X_{c5} = 70\%$.
B.7.2 Double order auxiliary controller.

X	α	G	ω_d
5.05	0.2510	−0.186225	1.8258

B.7.3 Induction machine data;
$r''_2 = 7.2 \times 10^{-4}$ pu, $x'_2 = 0.32646$ pu.

B.8 Mechanical system data: (at generator base).

$D_{ii} = 0$ for $i = 1–6$
$D_{ij} = 0$ for $i = 1–6, j = 1–6$

Mass	Shaft	Inertia (H) (s)	K (pu torque/rad)
HP		0.1033586	
	HP–IP		25.772
IP		0.1731106	
	IP–LPA		46.635
LPA		0.9553691	
	LPA–LPB		69.478
LPB		0.9837909	
	LPB–GEN		94.605
GEN		0.9663006	
	GEN–EXC		3.768
EXC		0.0380697	

References

[1] A. Ghosh, G. Ledwich, Modelling and control of TCSC, IEE Proc.-Gener. Transm. Distrb. 142 (3) (1995) 297–304.

[2] N. Kumar, M.P. Dave, Static var system auxiliary controllers for transient stability improvement of power systems, Electric Machines Power Syst. 24 (1996) 177–187.

[3] S.S. Choi, F. Jiang, G. Shrestha, Suppression of transmission system oscillations by TCSC, IEE Proc.-Gener. Transm. Distrib. 143 (1) (1996) 7–12.

[4] H.G. Han, J.K. Park, B.-H. Lee, Analysis of thyristor controlled series compensator dynamics using the static variable approach of a periodic system model, IEEE Trans. Power Deliv. 12 (4) (1997) 1744–1750.

[5] G. Li, T.T. Lie, G.B. shrestha, K.L. Lo, Design and application of coordinated multiple FACTS controllers, IEE Proc.-Gener. Transm. Distrib. 147 (2) (2000) 112–120.

[6] N. Yang, Q. Liu, J.D. McCalley, TCSC controller design for damping inter-area oscillations, IEEE Trans. Power Syst. 13 (4) (1998) 1304–1310.

[7] J.V. Milanovic, I.A. Hiskens, Damping enhancement by robust tuning of SVC controllers in the presence of load parameters uncertainty, IEEE Trans. Power Syst. 13 (4) (1998) 1298–1303.

[8] IEEE Special Stability Control Working Group, Static var compensator models for power flow and dynamics performance simulation, IEEE Trans. Power Syst. 9 (1) (1984) 229–240.

[9] R.S. Ramshaw, K.R. Padiyar, Generalized system model for slip-ring machines, IEE Proc., 120 (6), 1973.

[10] P.M. Anderson, et al., Subsynchronous Resonance in Power Systems, IEEE Press 1989.